

# Spatiotemporal fractal pattern in interfacial motion with quenched disorder

Ning-Ning Pang and N. Y. Liang

Department of Physics, National Taiwan University, Taipei, Taiwan, Republic of China

(Received 14 March 1997)

We study the recently introduced Leschhorn model [H. Leschhorn, *Physica A* **195**, 324 (1993)] for interfacial depinning with quenched disorder. The spatiotemporal intermittency observed in the system displays critical properties of fractals. By using the scaling argument, we are able to express various scaling exponents in terms of the fundamental exponents, i.e., the dynamical exponent  $z$ , the roughness exponent  $\chi$ , and the correlation length exponent  $\nu$ . Moreover, our simulation gives very good agreement with the prediction. The numerical values of various critical exponents show that the Leschhorn model is not in the same universality class of directed percolation. [S1063-651X(97)02108-9]

PACS number(s): 05.40.+j, 47.55.Mh, 64.60.Ht

Recently, there has been considerable interest in the scaling behaviors of interfaces in physical systems with quenched disorder, which are currently accepted as a prototype to describe the motion of a domain wall in the random field Ising model [1] and fluid displacement in porous media [2]. The simplest continuum description for the dynamics of the interface, proposed by Bruinsma and Aeppli [3] and Koplik and Levine [4], is given by the following Langevin equation:

$$\partial_t h(x, t) = \nu \nabla^2 h(x, t) + F + \eta(x, h(x, t)), \quad (1)$$

where  $F$  is a uniform driving force that pushes the interface  $h(x, t)$ , and the random term  $\eta(x, h(x, t))$  represents the effect of the quenched disorder. The random pinning force  $\eta(x, h(x, t))$  is Gaussian distributed with zero mean and some short spatial correlation length. Analytical [5] and numerical [6,7] studies showed that there exists a critical value of the force,  $F_c$ , above which the interface moves with a finite velocity; while below the transition the interface is pinned after some finite time. The depinning transition is continuous with the velocity of the interface  $v$ , playing the role of the order parameter, to vanish as a power law

$$v \sim (F - F_c)^\theta, \text{ as } F \rightarrow F_c^+. \quad (2)$$

The width  $w(L, t)$  of the kinetically roughened surface evolves in accordance with the dynamic scaling form

$$w^2(L, t) \equiv \overline{\langle (h(x, t) - \overline{h(x, t)})^2 \rangle} \sim L^{2\chi} f(t/L^z). \quad (3)$$

Here  $h(x, t)$  is the interface height at position  $x$  and time  $t$ . Throughout the paper, the overbar denotes the average over  $x$  in the system of size  $L$  at time  $t$ , and angular brackets denote the average over the randomness. In addition, for  $t \ll L^z$ ,  $w(L, t) \sim t^\beta$  with  $\beta = \chi/z$  and for  $t \gg L^z$ ,  $w(L, t) \sim L^\chi$ .  $\chi$  and  $z$  are known as the *roughness exponent* and the *dynamical exponent*, respectively.

In addition to the above standard scaling behavior of the interfacial width, the most intriguing feature of the interfacial onset through disordered media is that, at the depinning transition, the motion of the interface, rather than a more or less uniform growth, displays *spatiotemporal intermittency* [8]. That is, when a segment of the interface is pushed to become

unstable, it moves rapidly forward until it becomes pinned at some metastable state. Then the segment of the interface will remain stationary for a long while before it fails to adapt to the changing neighboring landscape and goes unstable again. Spatiotemporal intermittency is one of the most baffling phenomena observed in Nature. While spatiotemporal intermittency is observed in many physical systems, e.g., transition between turbulent and laminar flows in hydrodynamics [9], invasion percolation of the invading fluid (air) displacing oil from the oil reservoir [10], etc., little understanding about it has been achieved. This motivates us to study the  $(1+1)$ -dimensional Leschhorn model [11], which is the realization of Eq. (1) in a discrete space-time lattice. We explore many facets of the spatiotemporal intermittent behavior at the depinning transition of the system, including the waiting time distribution, the distribution of the size of pinned domains, and the corresponding spatial and temporal extents, etc.

Let us first recall the definition of the  $(1+1)$ -dimensional Leschhorn model [11]: (1) Each site on a square lattice is assigned a random pinning force  $\eta(i, h)$ , which takes the value 1 with probability  $p$  or  $-1$  with probability  $q = 1 - p$ . (2) The interface is specified by a set of integers  $h_i(t)$ ,  $i = 1, 2, \dots, L$ . The flat initial condition, i.e.,  $h_i(t=0) = 0$ , and periodic boundary conditions are imposed. (3) At each time step  $t$ , the interface configuration is updated simultaneously for all  $i$ :

$$h_i(t+1) = \begin{cases} h_i(t) + 1 & \text{if } v_i > 0 \\ h_i(t) & \text{otherwise;} \end{cases} \quad (4)$$

in the above expression, the value  $v_i$  is defined as

$$v_i = h_{i+1}(t) + h_{i-1}(t) - 2h_i(t) + g \eta(i, h). \quad (5)$$

The parameters  $g$  and  $q - p$  represent the relative strength of the random pinning force compared to the surface tension and the driving force, respectively. Reference [11] has shown that the mean interface height  $H(t) \equiv \langle \overline{h_i(t)} \rangle$  scales as  $t^\beta$  in the early times, then goes to a constant for  $p < p_c$  or grows linearly for  $p > p_c$ . Figure 1(a) shows a typical set of interface configurations  $h_i(t)$  separated with uniform time intervals  $\Delta t$  ( $= 200$  time steps) at the depinning transition

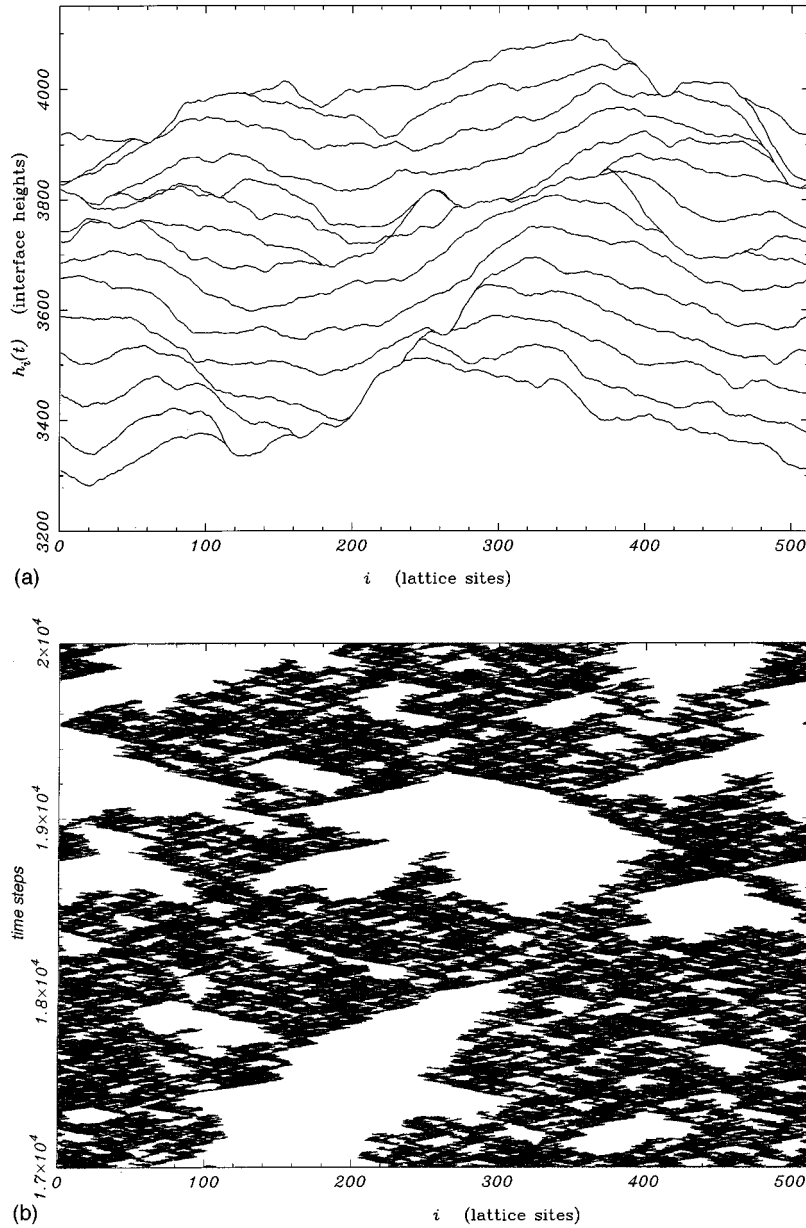


FIG. 1. (a) shows a typical set of interface configurations  $h_i(t)$  separated with uniform time intervals  $\Delta t$  (equals 200 time steps) at the depinning transition  $p_c (\approx 0.8004$ , for  $g=1$  [11]). Here the system size  $L=512$ . (b) shows the corresponding temporal evolution of interfacial motion. In (b), the moving sites at each time slice  $t$  are represented by black dots.

$p_c (\approx 0.8004$ , for  $g=1$  [11]). Here the system size  $L=512$ . The corresponding temporal evolution of interfacial motion is plotted in Fig. 1(b), where at each time  $t$  the moving sites are represented by black dots. Figure 1(b) clearly displays that, at the depinning transition, the motion of the interface is *intermittent* both in space and time. The pattern of activity looks like an anisotropic fractal in  $(1+1)$ - (one spatial and one temporal) dimensional space, of which the cuts in different directions have different fractal dimensions.

We first look at the cuts in the temporal direction. Let us define the *waiting time*  $\tilde{t}$  to be the time elapsed between the subsequent interfacial advance at a given site  $i$ .  $N_i(t)$  is defined as the total number of interfacial movement up to time  $t$ . Note that, from the fractal point of view,  $N_i(t)$  is the collection of the moving points on the time axis with the fractal dimension  $0 \leq \tilde{d} \leq 1$ . Then, on the average,

$$\langle \overline{N_i(t)} \rangle = t - \langle \overline{N_i(t)} \rangle \int_1^t \tilde{t} P_{\text{wait}}(\tilde{t}) d\tilde{t}, \quad (6)$$

where  $P_{\text{wait}}(\tilde{t})$  is the distribution of the waiting time  $\tilde{t}$ . It is evident that  $N_i(t) = h_i(t)$ , the interface height. In addition, the mean interface height  $H(t)$  scales as  $t^\beta$  in the early times [11], so we obtain

$$t^\beta \sim H(t) \equiv \langle \overline{h_i(t)} \rangle = \langle \overline{N_i(t)} \rangle \sim t^{\tilde{d}}. \quad (7)$$

Substituting Eq. (7) into Eq. (6), we obtain

$$1 + \int_1^t \tilde{t} P_{\text{wait}}(\tilde{t}) d\tilde{t} \sim t^{1-\tilde{d}}. \quad (8)$$

Consequently,

$$P_{\text{wait}}(\tilde{t}) \sim \tilde{t}^{-1-\tilde{d}}. \quad (9)$$

The waiting time distribution  $P_{\text{wait}}(\tilde{t})$  obeys the power-law behavior, with the exponent  $\tau_{\text{wait}}$  obtained as

$$\tau_{\text{wait}} = 1 + \tilde{d} = 1 + \beta = 1 + \chi/z. \quad (10)$$

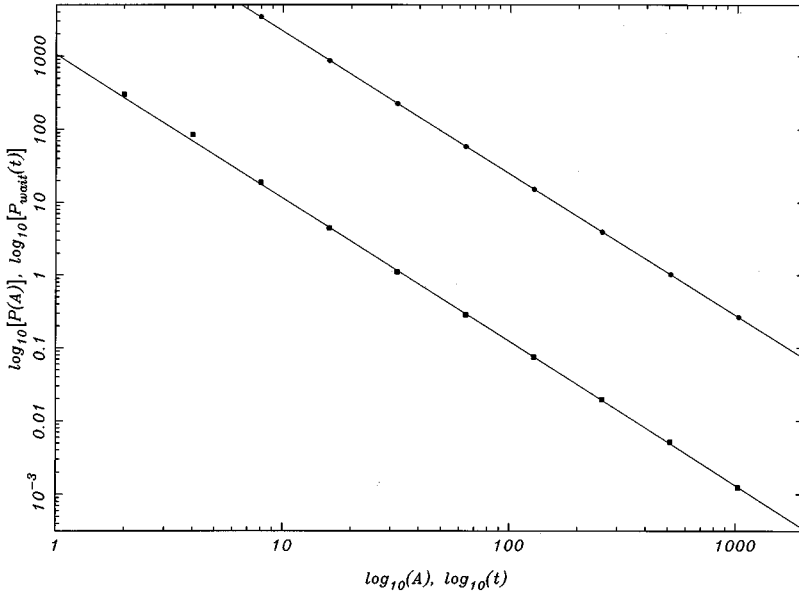


FIG. 2. The logarithmically binned distributions  $P_{\text{wait}}(\tilde{t})$  (solid square) and  $P(A)$  (solid circle), i.e., the density of events in the range  $[\tilde{t}, 2\tilde{t})$  and  $[A, 2A)$ , respectively. The numerically measured value of the waiting time distribution exponent  $\tau_{\text{wait}} = 2.0 \pm 0.1$  is in very good agreement with the predicted value  $\tau_{\text{wait}} = 1.88 \pm 0.06$ , based on the early-time exponent  $\beta = 0.88 \pm 0.03$  in Ref. [11]. The numerically measured value of the pinned domain area distribution exponent  $\tau = 2.0 \pm 0.1$  verifies our prediction of the scaling relation  $\tau \approx \tau_{\text{wait}}$ .

Subsequently, we look at the cuts in the spatial direction. The fractal dimension  $d_f$  of the collection of moving sites in the spatial direction, after long transients, can be related to the order parameter and correlation length exponents, i.e.,  $\theta$  and  $\nu$ , respectively, as follows. The velocity of the interface  $v$ , roughly speaking, scales as  $\tilde{N}(\xi)/\xi$ , where  $\tilde{N}(\xi)$  denotes the number of moving sites in the spatial range  $\xi$  at a given time slice, and  $\xi$  denotes the correlation length. Since

$$\tilde{N}(\xi) \sim \xi^{d_f} \quad (11)$$

and

$$\xi \sim (p - p_c)^{-\nu}, \quad (12)$$

with the help of Eq. (2) we obtain

$$\theta = \nu(1 - d_f). \quad (13)$$

Let us define  $P_{\text{syn}}(\tilde{l})$  as the distribution of the synchronization length  $\tilde{l}$ , which denotes the number of consecutive pinned sites at any given time step in the steady regime. In analogy with the cuts in the temporal direction, we can easily obtain

$$\tilde{N}(L) = L - \tilde{N}(L) \int_0^L P_{\text{syn}}(\tilde{l}) \tilde{l} d\tilde{l}, \quad (14)$$

where  $\tilde{N}(L)$  denotes the total number of moving sites in the spatial range  $L$  at a given time step. Substituting  $\tilde{N}(L) \sim L^{d_f}$  into Eq. (14), we obtain

$$1 + \int_0^L P_{\text{syn}}(\tilde{l}) \tilde{l} d\tilde{l} \sim L^{1-d_f}. \quad (15)$$

Consequently,

$$P_{\text{syn}}(\tilde{l}) \sim \tilde{l}^{-1-d_f}. \quad (16)$$

That is, the synchronization length distribution  $P_{\text{syn}}(\tilde{l})$  also obeys the power-law behavior with the exponent  $\tau_{\text{syn}}$  obtained as

$$\tau_{\text{syn}} = 1 + d_f = 2 - \theta/\nu. \quad (17)$$

We see that the cuts in either the temporal direction or the spatial direction can be regarded as fractal renewal processes [12], which are well known for generating  $1/f^D$  noises.

Moreover, the fractal pattern of space-time activities looks like a carpet with interwoven black (moving) and white (pinned) domains [see Fig. 1(b)]. We define pinned domains in  $x$ - $t$  space to be any group of pinned points that are connected through nearest-neighboring pinned points. The distribution of pinned domains with enclosed area  $A$ ,  $P(A)$ , obeys a power-law behavior at  $p_c$ . That is,

$$P(A) \sim A^{-\tau}. \quad (18)$$

Due to translational invariance in the  $x$  direction, the pinned domain can be viewed as a collection of the waiting time intervals of neighboring sites. The correlation between neighboring sites is introduced through the discrete Laplacian term, which favors the smoother interface, in the definition of the Leschhorn model. Thus  $\tau$  should be smaller than  $\tau_{\text{wait}}$ . However, since the interaction between neighboring sites is short ranged, more precisely the nearest-neighbor interaction, the model still preserves very good self-averaging quality. So we expect that  $\tau$  is smaller than but very close to  $\tau_{\text{wait}}$  within the range of statistical uncertainty in the numerical simulation. In addition, every pinned domain is characterized by a height  $r_{\perp}$  and a width  $r_{\parallel}$ , i.e., the projection of the domain in  $t$  and  $x$  directions, respectively. Since the dynamic exponent  $z$  measures the propagation of spatial correlations in time, we expect that  $r_{\perp} \sim r_{\parallel}^z$ . Because the hole is geometrically compact, the area  $A$  of the hole is of the order

$$A \sim r_{\parallel} r_{\perp} \sim r_{\parallel}^{1+z} \sim r_{\perp}^{1+1/z}. \quad (19)$$

By using

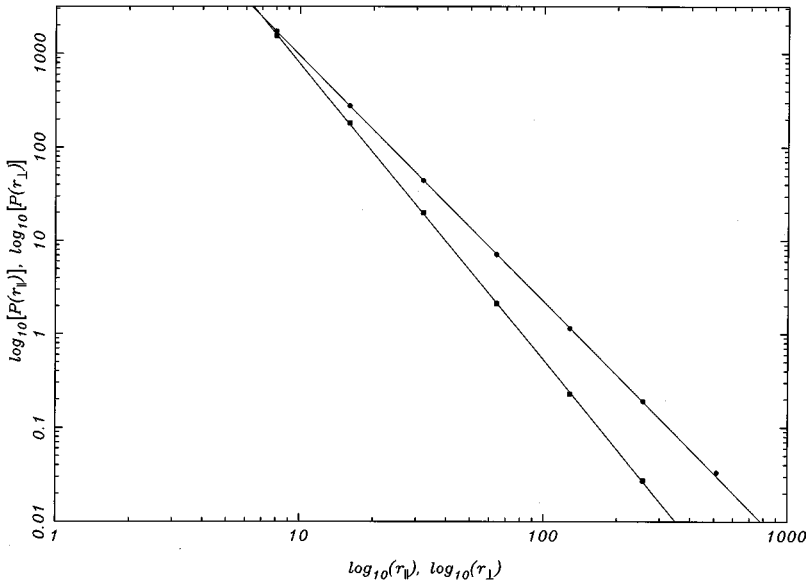


FIG. 3. The logarithmically binned distributions  $P(r_{\parallel})$  (solid square) and  $P(r_{\perp})$  (solid circle), i.e., the density of events in the range  $[r_{\parallel}, 2r_{\parallel})$  and  $[r_{\perp}, 2r_{\perp})$ , respectively. The straight lines, fit by least squares to the data, give  $\tau_{\parallel} = 3.2 \pm 0.3$  and  $\tau_{\perp} = 2.6 \pm 0.3$ , in excellent agreement with our theoretical predictions  $\tau_{\parallel} = 3.1 \pm 0.2$  and  $\tau_{\perp} = 2.5 \pm 0.1$ , based on the exponents  $\beta = 0.88 \pm 0.03$  and  $z = 1.4 \pm 0.1$  in Ref. [11].

$$P(r_{\parallel})dr_{\parallel} = P(r_{\perp})dr_{\perp} = P(A)dA, \quad (20)$$

we obtain the distributions of  $r_{\perp}$  and  $r_{\parallel}$  as  $P(r_{\parallel}) \sim r_{\parallel}^{-\tau_{\parallel}}$  and  $P(r_{\perp}) \sim r_{\perp}^{-\tau_{\perp}}$ , respectively, with the exponents

$$\tau_{\parallel} = \tau + \tau z - z = 1 + \chi + \chi/z \quad (21)$$

and

$$\tau_{\perp} = \frac{\tau + \tau z - 1}{z} = 1 + \chi/z + \chi/z^2. \quad (22)$$

We have obtained all the scaling exponents characterizing the fractal properties of the space-time activity pattern, in terms of the fundamental characteristic exponents, i.e., the roughness exponent  $\chi$ , the dynamic exponent  $z$ , and the correlation length exponent  $\nu$ .

We then perform numerical simulation to confirm our predictions. The simulation is done with the system size  $L = 512$  at  $p = p_c \approx 0.8004$ , and averaged over 5000 realizations. The typical time scale for systems to get pinned is around 20 000 time steps. Our numerical results strongly support the above scaling predictions. The numerically measured value of the waiting time distribution exponent  $\tau_{\text{wait}} = 2.0 \pm 0.1$ , displayed in Fig. 2, is in very good agreement with the predicted value  $\tau_{\text{wait}} = 1.88 \pm 0.06$ , based on the early time exponent  $\beta = 0.88 \pm 0.03$  in Ref. [11]. The expo-

nent  $\tau$ , characterizing the pinned domain area distribution, is also shown in Fig. 2. The numerical measurements,  $\tau = 2.0 \pm 0.1$  and  $\tau_{\text{wait}} = 2.0 \pm 0.1$ , verify our prediction of the scaling relation  $\tau \approx \tau_{\text{wait}}$ . Figure 3 shows that our numerical measurements,  $\tau_{\parallel} = 3.2 \pm 0.3$  and  $\tau_{\perp} = 2.6 \pm 0.3$ , are in excellent agreement with our theoretical predictions,  $\tau_{\parallel} = 3.1 \pm 0.2$  and  $\tau_{\perp} = 2.5 \pm 0.1$ , based on the exponents  $\beta = 0.88 \pm 0.03$  and  $z = 1.4 \pm 0.1$  in Ref. [11].

In conclusion, we studied the recently introduced Leschhorn model for interfacial depinning with quenched disorder. We first applied the method of scaling analysis to study the scaling properties of the spatiotemporal fractal pattern of activities observed in the  $(1+1)$ -dimensional Leschhorn model. We derived the relations between various scaling exponents analytically. Moreover, an extensive numerical simulation was undertaken to affirm our predictions about scaling relations. The numerical values of various critical exponents show that the Leschhorn model is not in the same universality class of directed percolation, although the pattern of activity is indeed visually similar to that of directed percolation.

The authors are very grateful to C. K. Chan and W. J. Tzeng for enlightening discussions. The work of N.-N. Pang is supported in part by the National Science Council of Republic of China under Grant No. NSC 86-2112-M-002-021.

- 
- [1] H. Ji and M. Robbins, Phys. Rev. B **46**, 14 519 (1992).
  - [2] N. Martyts and M. Robbins, Phys. Rev. B **44**, 12 294 (1992).
  - [3] R. Bruinsma and G. Aeppli, Phys. Rev. Lett. **52**, 1547 (1984).
  - [4] J. Koplik and H. Levine, Phys. Rev. B **32**, 280 (1985).
  - [5] T. Nattermann, S. Stepanow, L.-H. Tang, and H. Leschhorn, J. Phys. (France) II **2**, 1483 (1992).
  - [6] G. Parisi, Europhys. Lett. **17**, 673 (1992).
  - [7] S. Roux and A. Hansen, J. Phys. (France) I **4**, 515 (1994).
  - [8] L.-H. Tang, in *Annual Reviews of Computational Physics II*,

- edited by D. Stauffer (World Scientific, Singapore, 1995).
- [9] See, for example, *Hydrodynamic Instabilities and the Transition to Turbulence*, edited by H. L. Swinney and J. P. Gollub (Springer-Verlag, Berlin, 1981).
- [10] R. Lenormand and C. Zarcione, Phys. Rev. Lett. **54**, 2226 (1985).
- [11] H. Leschhorn, Physica A **195**, 324 (1993).
- [12] S. B. Lowen and M. C. Teich, Phys. Rev. E **47**, 992 (1993).